

## Raman coherence beats from the entangled state involving polarized excitons in single quantum dots

Xiaoqin Li,<sup>1</sup> Yanwen Wu,<sup>1</sup> D. G. Steel,<sup>1</sup> D. Gammon,<sup>2</sup> and L. J. Sham<sup>3</sup>

<sup>1</sup>Harrison M. Randall Laboratory of Physics, The University of Michigan, Ann Arbor, Michigan 48109-1120, USA

<sup>2</sup>Naval Research Laboratory, Washington, D.C. 20375-5347, USA

<sup>3</sup>Department of Physics, The University of California, San Diego, La Jolla, California 92093-0319, USA

(Received 25 May 2004; published 19 November 2004)

The optically induced and detected entangled state involving an exciton Zeeman doublet with entanglement entropy as high as  $\sim 0.7$  was created using picosecond lasers in single GaAs quantum dots. The temporal evolution of the nonradiative Raman coherence between two exciton states was directly resolved in quantum beats measured in the homodyne detected differential transmission experiment. The Raman coherence time,  $66 \pm 15$  ps, was determined from the decay of the envelope of the quantum beats, and was found to be limited by the lifetimes of the exciton transitions,  $50 \pm 3$  ps.

DOI: 10.1103/PhysRevB.70.195330

PACS number(s): 78.67.Hc, 03.67.Lx, 42.50.Hz, 42.50.Md

An interesting prospect in nanoscience is the control of quantum operations in nanosystems. We report here experimental progress in the optical control of quantum operations in a single semiconductor quantum dot to generate entangled states. A state of a pair of quantum systems is said to be entangled if it is not factorizable into the states of the individual systems. Entanglement is a quintessential quantum property. It is an essential ingredient in rendering the quantum information processing superior to the classical counterpart.<sup>1</sup> Entangled quantum states have been studied for photons<sup>2</sup> and massive particles.<sup>3,4</sup> Studies performed on solid state qubits are particularly interesting due to their potential in building integrated devices.<sup>5-7</sup>

Controlling and detecting the entanglement between a pair of qubits is a basic requirement for building model quantum information processing devices based on dipole transitions in quantum dot (QD) structures. In single QD's, Bloch vectors of two nondegenerate interacting excitons with orthogonal polarizations can be used as two distinguishable qubits.<sup>8-10</sup> This two-bit system shown in Fig. 1 involves the ground state ( $|00\rangle$ ), two exciton states ( $|01\rangle$  and  $|10\rangle$ ) and the biexciton state ( $|11\rangle$ ) where the value 0 (1) represents the absence (presence) of an exciton corresponding to the optical Bloch vector pointing down (up). While an entangled state of two qubits separated in different dots is most useful, the general spectroscopy features explored in our model system can be applied to more complex scalable systems.<sup>11-14</sup>

A two-qubit logic gate based on a single QD has been demonstrated<sup>15</sup> recently as the controlled rotation (CROT) of one qubit conditioned on the *presence* of the other qubit. We utilize the strong exciton-exciton interaction to produce an entangled state using an operation equivalent to a sequence of two CROT's of one qubit conditioned on the *absence* of the other qubit. Our approach involves only one excitation pulse with appropriate polarization and pulse area. It is simpler and more effective compared to applying two sequential logic gates. Experimental demonstrations of exciton and biexciton Rabi oscillations<sup>15,16</sup> provided evidence that the relatively high excitation and broad optical bandwidth needed for qubit rotations also lead to coupling to nearby

states resulting in unintended dynamics and possible errors in computation. The current study shows entangled states involving the Zeeman doublet  $|01\rangle$  and  $|10\rangle$  can be created and maintained under these conditions.

A quantitative measure of entanglement,<sup>17</sup> known as the entanglement of formation  $E$ , is the von Neumann entropy of the reduced density matrix of either of the two subsystems for a pure state.<sup>18</sup> An earlier experiment, performed at extremely low excitation level with ultranarrow bandwidth (nano-eV) laser sources, created weakly entangled states<sup>5</sup> with  $E=0.08$ . We report here an entanglement of  $E=0.7$  for an operation designed to produce the maximal entanglement of 1. The capability of creating an entangled pair of qubits with large entropy means that more information can be carried by such a pair of qubits and is, thus, important for quantum information processing based on semiconductor QD's.

It is noteworthy that the previous demonstration of a CROT operation<sup>15</sup> requires only the dipole coherence while the creation of an entangled state depends on the nonradiative coherence between the two exciton transitions. These two different coherence times govern the dynamics of two distinctive terms in the density matrix used to describe the quantum system. Full characterization of the density matrix is essential for a complete understanding of the quantum

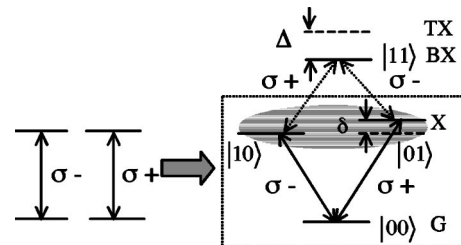


FIG. 1. In the presence of a modest magnetic field applied along the growth direction, two excitons with orthogonal polarizations can be excited within a single dot. In the excitation picture, G, X, BX, and TX represent the crystal ground state, the exciton, the biexciton and the virtual two-exciton state, respectively. The biexciton binding energy,  $\Delta$ , is much larger than the laser bandwidth. Therefore, the problem is reduced to a V system enclosed in the box.

dynamics of the system subject to logic operations. This paper has made a step forward towards such a complete characterization by demonstrating the possibility of measuring the nonradiative coherence term under the same conditions required by gate operations.

Quantum beats measured in the homodyne detected differential transmission (DT) geometry as well as in the time resolved photoluminescence<sup>19,20</sup> have proven to be a powerful spectroscopy tool to study the nonradiative coherence between electronic superposition states. Quantum beats arise from two electronic states nearly degenerate in energy that are simultaneously excited by a laser field with the proper polarization and sufficient bandwidth. During the light-matter interaction, the optical coherence is transferred to the quantum coherence between the coupled states. In the homodyne detection of the DT geometry, the time evolution of the phase of the coherent superposition of the two states is directly detected. Most previous studies are performed on bulk materials, quantum wells, and ensembles of self-assembled quantum dots, where the decay of the quantum beats is usually limited by inhomogeneous broadening.<sup>20–22</sup> In a previously reported luminescence detected quantum beat experiment performed on single CdSe nanocrystals, coherence between the exciton fine structure doublets was studied.<sup>23</sup> It was hypothesized that such coherence was partially maintained during population relaxation processes from the excited states.

The resonant excitation nature of the DT measurement utilized in this study enables the direct measurement of the nonradiative coherence time between states  $|01\rangle$  and  $|10\rangle$  (referred to as Raman coherence). The temporal evolution of the nonradiative Raman quantum coherence was observed as a damped oscillatory signal with a frequency determined by the energy splitting of the exciton Zeeman doublet. The Raman coherence time was determined from the decay of the oscillation envelope and was found to be limited by the lifetimes of exciton transitions consistent with the previous weak field study.<sup>5</sup> This consistency between the strong and weak field behavior highlights a fundamental difference and a main advantage of an ultimate quantum confined system offered by a single quantum dot compared to a higher dimensional system such as quantum well. It has been shown by numerous experiments that the nature and signature of many-body interactions in quantum wells change as the optical excitation power is increased.<sup>24</sup> The current study indicates that quantum dynamics in QD's have been dramatically changed by the three-dimensional confinement and are well described by simple atomic models even under logic gate operation conditions in the strong field regime, therefore, justifying the choice of quantum dots as a primary candidate for solid-state based quantum information processing devices.

In a single QD, quantum confinement greatly enhances the effect of the Coulomb interaction, leading to the formation of the biexciton state comprised of two orthogonally polarized excitons. The excitation of one exciton affects the resonant energy of the other, which corresponds to the characteristic conditional quantum dynamics needed for quantum computing. In the absence of interaction between two excitons, quantum beats in DT measurements disappear.<sup>20</sup> The

biexciton has a binding energy ( $\sim 3.5$  meV) much larger than the bandwidth of the laser ( $\sim 0.4$  meV) as a result of the strong Coulomb interaction. Therefore it can be safely ignored in the excitation process.<sup>25</sup>

The problem can be simplified to a three-level V system coupled to the optical fields shown in Fig. 1. The proper formalism to describe the quantum dynamics of the V system is based on the master equation for the density matrix operators,

$$i\hbar \frac{d\rho}{dt} = [H, \rho] + i\hbar \left. \frac{d\rho}{dt} \right|_{\text{relaxation}}, \quad (1)$$

where  $H = H_0 + V = H_0 - \hat{\mu} \cdot \mathbf{E}$ , the first term corresponds to the diagonalized Hamiltonian for the eigenstates of the excitation level diagram and the second term describes the coherent coupling of the laser field. The nonzero elements of the dipole moment operator correspond to the transitions labelled in Fig. 1. The last term in Eq. (1) is a generalized decay operator that accounts for the population decay of different states (the diagonal density matrix terms) and the dephasing of the optically induced coherence (the off-diagonal density matrix terms). The solutions to the master equations in the case of a V system are well understood.<sup>26</sup>

There are two different types of terms contributing to the third order nonlinear signal. One results from population saturation effects, which goes through the perturbation paths such as

$$\rho_{00,00}^{(0)} \xrightarrow{E_1^*} \begin{Bmatrix} \rho_{00,10}^{(1)} \\ \rho_{00,01}^{(1)} \end{Bmatrix} \xrightarrow{E_1} \begin{Bmatrix} \rho_{10,10}^{(2)} \\ \rho_{01,01}^{(2)} \end{Bmatrix} \xrightarrow{E_2^*} \begin{Bmatrix} \rho_{00,10}^{(3)} \\ \rho_{00,01}^{(3)} \end{Bmatrix}. \quad (2)$$

These terms include the diagonal terms at the second order in the perturbation theory. Another class of terms are the so-called coherent terms which go through the perturbation paths such as

$$\rho_{00,00}^{(0)} \xrightarrow{E_1^*} \begin{Bmatrix} \rho_{00,10}^{(1)} \\ \rho_{00,01}^{(1)} \end{Bmatrix} \xrightarrow{E_1} \rho_{10,01}^{(2)} \xrightarrow{E_2^*} \begin{Bmatrix} \rho_{00,10}^{(3)} \\ \rho_{00,01}^{(3)} \end{Bmatrix}. \quad (3)$$

There are only off-diagonal density matrix terms in the perturbation path. The nonradiative Raman coherence is related to the coherent terms, seen at the second order. It manifests itself in an oscillatory signal with frequency determined by the energy splitting between states  $|01\rangle$  and  $|10\rangle$ .

The interface fluctuation QD's are formed in a 4.2 nm GaAs/Al<sub>0.3</sub>Ga<sub>0.7</sub>As layer, and are probed with high spatial resolution through submicron apertures on an Al mask deposited on the sample surface.<sup>27</sup> The dot potential tends to be elongated along the  $[110]$  crystal axis which leads to an exciton fine structure splitting with linear optical selection rules.<sup>28</sup> A magnetic field applied in the Faraday geometry of modest strength ( $\sim 0.85$  Tesla) restores the circular selection rules of the exciton Zeeman transitions as indicated in Fig. 1.

In degenerate DT measurements, the pump  $[\mathbf{E}_1(t), \omega_1]$  and the probe  $[\mathbf{E}_2(t), \omega_2 = \omega_1, \text{delayed from the pump by } \tau]$  were derived from the same laser. The pulsed laser was adjusted to have a pulse width of  $\sim 5$  ps and bandwidth  $\sim 0.4$  meV, which is wide enough to cover both exciton Zeeman states at the magnetic field applied but narrow enough

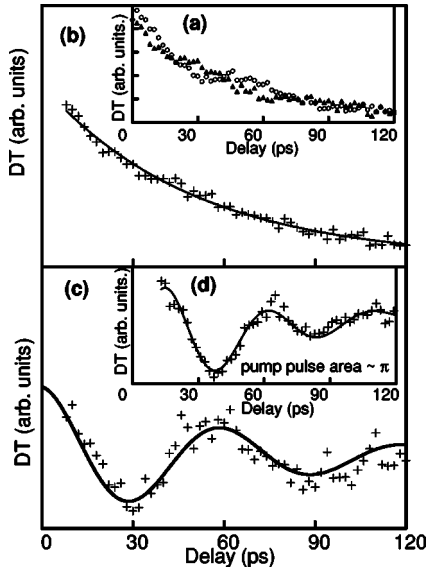


FIG. 2. (b) Sum and (c) difference of the  $DT_{CLP}$  and  $DT_{OLP}$  with the original data shown in (a). Solid lines are theoretical fits to the data with an exponential function in (b) and a decaying cosine function in (c). The data shown in (d) is obtained in similar experiments with a higher pump power. The Raman coherence time is reduced at higher excitation power most likely due to the increased scattering of the resonantly excited exciton from nearly degenerate delocalized states (Ref. 16).

to selectively excite single QD's. Both beams were focused onto the same aperture on the sample held at 6 K. Two acoustic optical modulators (AOM) were used to intensity modulate both beams at  $\sim 1$  MHz. The nonlinear polarization signal field was then homodyne detected with the transmitted laser beam and sent to a lock-in amplifier. If the laser frequency is scanned with the delay between the pump and probe fixed around zero, single exciton resonances can be mapped out.<sup>29</sup> For the current experiments, the laser frequency was tuned to one of the resonances and the delay was varied to study the dynamics as discussed in details below.

If the polarizations of the pump and probe beams were chosen to be cocircularly polarized, the beams were coupled to only one of the Zeeman transitions. The DT signal as a function of delay was a smooth exponential decay. The decay constant is the lifetime of the corresponding transition (data not shown). If, however, the pump and probe beams were linearly polarized so that both beams were coupled to the two exciton Zeeman transitions simultaneously, a characteristic beating signal appeared on top of the exponential decay as shown in Fig. 2(a). Pump and probe beams with colinear polarization and orthogonal-linear polarization were used to obtain the curves with circles and triangles, respectively. An oscillatory behavior was observed in both polarization configurations with a phase difference between them.

The nonlinear polarization field calculated from solving Eq. (1) is used in the optical Bloch equations to find the homodyne detected DT signal for both colinearly polarized and orthogonal-linearly polarized pump and probe fields. The population relaxation time of both exciton states is  $\Gamma$ , and the Raman coherence time (the decay time of the off-diagonal

term  $\rho_{10,01}$ ) is  $\gamma_{10,01}$ . Spin relaxation time between states  $|01\rangle$  and  $|10\rangle$  is longer than the time scales of interest here and therefore is neglected in the current discussion.<sup>30-32</sup> The DT signals for the colinear polarization ( $DT_{CLP}$ ) and orthogonal linear polarization ( $DT_{OLP}$ ) are calculated as follows:

$$DT_{CLP}(\tau) \propto [3e^{-\Gamma\tau} + e^{-\gamma_{10,01}\tau} \cos(\delta\tau)]\Theta(\tau), \quad (4)$$

$$DT_{OLP}(\tau) \propto [3e^{-\Gamma\tau} - e^{-\gamma_{10,01}\tau} \cos(\delta\tau)]\Theta(\tau). \quad (5)$$

The sum of the  $DT_{CLP}$  and  $DT_{OLP}$  is displayed in Fig. 2(b). It fits to an exponential function and yields the population relaxation time of the exciton transitions,  $\Gamma^{-1} = 50 \pm 3$  ps, in agreement with measurements using colinearly polarized light. The difference of the  $DT_{CLP}$  and  $DT_{OLP}$  is displayed in Fig. 2(c) where a cosine function with decaying envelope is fit to the data. The Raman period ( $T_R$ ) and the energy splitting between the Zeeman doublet ( $\hbar\delta$ ) are related by  $T_R\delta = 2\pi$ . The Raman period,  $T_R$ , obtained from the curve fit is  $\sim 60$  ps, which corresponds to an energy splitting between the Zeeman states of  $\hbar\delta = 55 \mu\text{eV}$ . The energy splitting can be related to the exciton  $g$  factor by  $\hbar\delta = |g_{ex}| \mu_B B$  as verified in both ensemble and single state measurements, where  $\mu_B$  is the Bohr magneton, and  $B$  is the magnetic field. The exciton  $g$  factor,  $|g_{ex}|$ , is then calculated to be 1.1, comparable to previous studies.<sup>33</sup> The coherence time between the Zeeman doublet,  $\gamma_{10,01}^{-1} = 66 \pm 15$  ps, is extracted from the decay of the envelope. The following relation exists between  $\gamma_{10,01}$  and the population relaxation rate of the exciton Zeeman states ( $\Gamma$ ):  $\gamma_{10,01} = [(\Gamma_{01} + \Gamma_{10})/2] + \gamma_{\text{pure}}$ , where  $\gamma_{\text{pure}}$  represents the nonradiative coherence decay rate due to pure dephasing processes. Considering  $\gamma_{10,01}^{-1} = 66 \pm 15$  ps and  $\Gamma_{01}^{-1} \approx \Gamma_{10}^{-1} = 50 \pm 3$  ps, we come to the conclusion that the Raman coherence is limited by the lifetimes of the exciton transitions involved, which is consistent with the previous study in the frequency domain.<sup>5</sup>

In the order of increasing complexity, we first treat the quantum state of the system as a pure state approximately and quantify the entanglement using the von Neumann entropy. The complete wave function immediately following the pump pulse can be written as  $|\Psi\rangle = C_0|00\rangle + C_+|01\rangle + C_-|10\rangle + C_{+-}|11\rangle$ , where the two qubits correspond to the Bloch vectors of two orthogonally polarized excitons. When the coefficients satisfy the relation  $C_{+-} = C_-C_+/C_0$ , the state is factorizable. Otherwise, the state is an entangled state in the Bloch vector basis. Since the excitation of the state  $|11\rangle$  is negligibly small due to the large binding energy of the biexciton,  $C_{+-} \sim 0$ . The single exciton Rabi oscillation experiment<sup>16</sup> is repeated using circularly polarized light to measure the power corresponding to a  $\pi$  pulse with the shape and time duration specified earlier. Then, in the experiment shown in Fig. 2(d), a linear polarized light with twice that power is chosen. Thus, the pump pulse coupling the ground state to each exciton Zeeman state has a pulse area  $\sim \pi$ . The measured population of the exciton state is  $0.77 \pm 0.06$  under a  $\pi$  pulse.<sup>34</sup> Assuming states  $|01\rangle$  and  $|10\rangle$  are equally excited and their population sums up to 0.77, the coefficients for the wave function following the pump pulse are estimated to be  $C_0 = 0.48$ ,  $C_+ = C_- = 0.62$ ,  $C_{+-} = 0$ , leading to a von Neumann

entropy of entanglement  $E \sim 0.7$ .<sup>18</sup> The chosen pulse area is designed to produce under idealized circumstances the maximally entangled Bell state  $(|01\rangle + |10\rangle)/\sqrt{2}$  with an entanglement of unity. Quantum dephasing processes, mostly population relaxation in the system under current studies, lead to deviation from the maximally entangled state.

A more accurate analysis describes the quantum state following the pump pulse as a mixed state due to the presence of dephasing. For a mixed state, the statistical properties of the mixture can hide the quantum correlations such that even the distinction between separable and entangled systems becomes very difficult. However, in the case of a bipartite system, it is possible to compute explicitly the entanglement of formation once the density matrix describing the quantum

state is known.<sup>35</sup> The experimental reconstruction of the full density matrix is an important problem under current investigation. For now, we calculate the density matrix describing the state of the two-bit system following the pump pulse by solving the density matrix equations with typical dephasing times ( $T_1 = T_2 = 50$  ps; in reality,  $T_2$  is usually longer than  $T_1$  in the QD's under the study) and pulse shapes [ $E \propto \text{sech}(t/T)$ ,  $T \sim 3$  ps] included. The entanglement of formation using the density matrix calculated at 5 ps (10 ps) following the peak of the pump pulse is  $\sim 0.8$  (0.7).

This work was supported by the ONR, ARDA, ARO, NSA, AFOSR, NSF, and DARPA/Spins.

- 
- <sup>1</sup>A. Ekert and R. Jozsa, *Rev. Mod. Phys.* **68**, 733 (1996).
- <sup>2</sup>See the review by A. Zeilinger, *Rev. Mod. Phys.* **71**, S288 (1999).
- <sup>3</sup>E. Hagley, X. Maitre, G. Nogues, C. Wunderlich, M. Brune, J. M. Raymond, and S. Haroche, *Phys. Rev. Lett.* **79**, 1 (1997).
- <sup>4</sup>Q. A. Turchette, C. S. Wood, B. E. King, C. J. Myatt, D. Leibfried, W. M. Itano, C. Monroe, and D. J. Wineland, *Phys. Rev. Lett.* **81**, 3631 (1998).
- <sup>5</sup>G. Chen, N. H. Bonadeo, D. G. Steel, D. Gammon, D. S. Katzer, D. Park, and L. J. Sham, *Science* **289**, 1906 (2000).
- <sup>6</sup>M. Bayer, P. Hawrylak, K. Hinzer, S. Fafard, M. Korkusinski, Z. R. Wasilewski, O. Stern, and A. Forchel, *Science* **291**, 451 (2001).
- <sup>7</sup>Yu. A. Pashkin, T. Yamamoto, O. Astafiev, Y. Nakamura, D. V. Averin, and J. S. Tsai, *Nature (London)* **421**, 823 (2003).
- <sup>8</sup>A. Barenco, D. Deutsch, A. Ekert, and R. Jozsa, *Phys. Rev. Lett.* **74**, 4083 (1995).
- <sup>9</sup>F. Troiani, U. Hohenester, and E. Molinari, *Phys. Rev. B* **62**, R2263 (2000).
- <sup>10</sup>P. Chen, C. Piermarocchi, and L. J. Sham, *Phys. Rev. Lett.* **87**, 067401 (2001).
- <sup>11</sup>A. Imamoglu, D. D. Awschalom, G. Burkard, D. P. DiVincenzo, D. Loss, M. Sherwin, and A. Small, *Phys. Rev. Lett.* **83**, 4204 (1999).
- <sup>12</sup>E. Biolatti, R. C. Iotti, P. Zanardi, and F. Rossi, *Phys. Rev. Lett.* **85**, 5647 (2000).
- <sup>13</sup>C. Piermarocchi, P. Chen, L. J. Sham, and D. G. Steel, *Phys. Rev. Lett.* **89**, 167402 (2002).
- <sup>14</sup>G. Burkard, D. Loss, and D. P. DiVincenzo, *Phys. Rev. B* **59**, 2070 (1999).
- <sup>15</sup>X. Li, Y. Wu, D. G. Steel, D. Gammon, T. H. Stievater, D. S. Katzer, D. Park, C. Piermarocchi, and L. J. Sham, *Science* **301**, 809 (2003).
- <sup>16</sup>T. H. Stievater, X. Li, D. G. Steel, D. Gammon, D. S. Katzer, D. Park, C. Piermarocchi, and L. J. Sham, *Phys. Rev. Lett.* **87**, 133603 (2001).
- <sup>17</sup>C. H. Bennett, D. P. DiVincenzo, J. A. Smolin, and W. K. Wootters, *Phys. Rev. A* **54**, 3824 (1996).
- <sup>18</sup>Von Neumann entropy for a pure state  $\Psi$  of a bipartite system is defined as  $E(\Psi) = -\text{Tr}(\rho_A \log_2 \rho_A)$ , where  $\rho_A$  is the partial trace of  $|\Psi\rangle\langle\Psi|$  over the subsystem  $B$ . For a mixed state,  $\rho = \sum_i p_i |\Psi_i\rangle\langle\Psi_i|$ , the entanglement of formation is defined as the average entanglement of the pure states of the decomposition, minimized over all decompositions of  $\rho$ .  $E(\rho) = \min \sum_i p_i E(\Psi_i)$ .
- <sup>19</sup>V. Langer, H. Stolz, and W. von der Osten, *Phys. Rev. Lett.* **64**, 854 (1990).
- <sup>20</sup>K. B. Ferrio and D. G. Steel, *Phys. Rev. Lett.* **80**, 786 (1998).
- <sup>21</sup>K. Leo, J. Shah, E. O. Gobel, T. C. Damen, S. Schmitt-Rink, W. Schafer, and K. Kohler, *Phys. Rev. Lett.* **66**, 201 (1991).
- <sup>22</sup>A. S. Lenihan, M. V. Gurudev Dutt, D. G. Steel, S. Ghosh, and P. K. Bhattacharya, *Phys. Rev. Lett.* **88**, 223601 (2002).
- <sup>23</sup>T. Flissikowski, A. Hundt, M. Lowisch, M. Rabe, and F. Henneberger, *Phys. Rev. Lett.* **86**, 3172 (2001).
- <sup>24</sup>D. S. Chemla and J. Shah, *Nature (London)* **411**, 549 (2001).
- <sup>25</sup>G. Chen, T. H. Stievater, E. T. Batteh, Xiaoqin Li, D. G. Steel, D. Gammon, D. S. Katzer, D. Park, and L. J. Sham, *Phys. Rev. Lett.* **88**, 117901 (2002).
- <sup>26</sup>P. Meystre and M. Sargent, *Elements of Quantum Optics*, 3rd ed. (Springer-Verlag, New York, 1999).
- <sup>27</sup>D. Gammon, E. S. Snow, B. V. Shanabrook, D. S. Katzer, and D. Park, *Science* **273**, 87 (1996).
- <sup>28</sup>D. Gammon, E. S. Snow, B. V. Shanabrook, D. S. Katzer, and D. Park, *Phys. Rev. Lett.* **76**, 3005 (1996).
- <sup>29</sup>T. H. Stievater, X. Li, D. G. Steel, D. Gammon, D. S. Katzer, and D. Park, *Phys. Rev. B* **65**, 205319 (2002).
- <sup>30</sup>H. Gotoh, H. Ando, H. Kamada, A. Chavez Pirson, and J. Temmyo, *Appl. Phys. Lett.* **72**, 1341 (1998).
- <sup>31</sup>M. Paillard, X. Marie, P. Renucci, T. Amand, A. Jbeli, and J. M. Gerard, *Phys. Rev. Lett.* **86**, 1634 (2001).
- <sup>32</sup>T. H. Stievater, X. Li, T. Cubel, D. G. Steel, D. Gammon, D. S. Katzer, and D. Park, *Appl. Phys. Lett.* **81**, 4251 (2002).
- <sup>33</sup>G. Chen, Ph.D. thesis, Ann Arbor, MI, 2002.
- <sup>34</sup>X. Li, Ph.D. thesis, Ann Arbor, MI, 2003.
- <sup>35</sup>W. K. Wootters, *Phys. Rev. Lett.* **80**, 2245 (1998).